Journal of Materials Chemistry B

Accepted Manuscript

ROYAL SOCIETY OF CHEMISTRY

www.rsc.org/materialsB

Journal of Materials Chemistry B

ARTICLE

Folic Acid-Tethered Poly(*N*-isopropylacrylamide)–Phospholipid Hybrid Nanocarrier for Targeted Drug Delivery

Received 00th January 20xx,
Accepted 00th January 20xx

DOI: 10.1039/x0xx00000x

www.rsc.org/

Johnson V John,[a] Young-Il Jeong,[b] Renjith P. Johnson,[a] Chung-Wook Chung,[b] Huiju Park,[a] Dae Hwan Kang,[b] Jin Ku Cho,[c] Yongjin Kim[c] and Il Kim*[a]

A series of temperature-responsive lipopolymers have been synthesized by bioconjugating poly(*N*-isopropylacrylamide)$_n$ (n = 25, 40, 60) onto three different phospholipids by the combination of reversible addition fragmentation chain transfer polymerization and azide-alkyne click reactions. To achieve the active targeting of cancer cells, folic acid (FA) has also been tethered to the resulting hybrid materials. The doxorubicin (Dox) encapsulated uniform nanocarriers (150 nm in diameter) fabricated by the self-assembly of the lipopolymers display temperature responsive controlled release. The FA receptor-mediated delivery of Dox was then assessed by using KB cell lines, and the anti-cancer activity was assessed by the blocking of folic acid receptors. The FA-tethered lipopolymers showing temperature-responsiveness is advantageous for the cell-specific release of Dox, potentiating the anti-cancer activity.

Introduction

Polymeric nanocarriers (PNCs) have gained considerable attention in the last two decades as a multifunctional delivery system for poorly water-soluble drugs. Nanoscopic size, ability to solubilize hydrophobic drugs in large amounts and achieve site-specific delivery have made them as promising candidates to achieve desirable biopharmaceutical and pharmacokinetic properties of drugs and enhance their bioavailability. In general PNCs have been accumulated in tumor tissues either by passive or active targeting mechanism.[1,2] Passive targeting PNCs always provide the low therapeutic index into the diseased tissues via enhanced permeability and retention effect (EPR). Additionally, during the circulation drug leakage has been occurred due to the lack of targetability.[2] Targeting species incorporated stimuli-responsive PNCs may reduce the drug leakage because they can release the anticancer agents based on the intra- or extracellular environments in the targeted diseased sites.[3,4] Various types of biocompatible polymers and synthetic polymer bioconjugates have been extensively studied for the fabrication PMs in the last decade.[5] Phospholipid (PL) conjugated polymers have attracted great interest for the synthesis of PNCs. 2-Methacryloyloxyethyl phosphorylcholine bearing copolymers,[6] PLs end-capped polyurethanes,[7] PLs bearing polypeptides and other PLs-lipid mimic hybrids[8,9] are the typical examples.

Since the first discovery by Bangham in 1965 and the first liposomal chemotherapeutic product (Doxil®) in 1995,[10-13]PLs have been widely applied as drug carriers in clinic due to their superior features, particularly biocompatibility, biodegradability, low toxicity and structural variability. Currently, there are lots of liposome-based drugs approved for clinical use and more are in various stages of clinical trials.[11,14] For the active intake of drugs in the diseased sites considerable effort has been made on the new generation liposomes, such as temperature sensitive liposomes (ThermoDox®), cationic liposomes (EndoTAG1-1®), virosomes (Expal® and Inflexal V®), and PEGylated liposomes (Doxil® and Lipo-dox®) has progressed by modulating the preparation techniques and lipid composition. The PEG-ylated liposomes modified by incorporating hydrophilic polyethylene glycol (PEG) in the bilayer[15]are known to provide stabilization enhancement and additional protection of the encapsulated drugs as well as enhanced circulation half-life *in vivo*. However, PEGylated liposomes displayed significant incidence of stomatitis in clinical trials. In addition, most of the new generation liposomes showed no dramatic improvements in therapeutic efficiency compared with free drug or conventional liposomes. For example, ThermoDox® displayed significantly weaker doxorubicin accumulation in mice tumors after a day of administration in comparison with Doxil.[16]

Usually, PL-PEG and PL-PEG-folic acid (FA) is common ingredient for the liposomal formulation even though they don't have any stimuli responsiveness. Recently, Liu *et al.*[17] developed a nanoparticle of mixed lipid monolayer containing

[a] *BK21 PLUS Center for Advanced Chemical Technology, Department Polymer Science and Engineering, Pusan National University, Pusan 609-735, Republic of Korea*
[b] *Biomedical Research Institute, Pusan National University Hospital, Pusan 602-739, Republic of Korea*
[c] *Green Process and Materials R&D Group, Korea Institution of Industrial Technology, 89 Yangdaegiro-gil, Ipjang-myeon, Cheonan 331-822, Republic of Korea*

† Footnotes relating to the title and/or authors should appear here.
Electronic Supplementary Information (ESI) available: [details of any supplementary information available should be included here]. See DOI: 10.1039/x0xx00000x

PL-PEG, PL-PEG-FA and biodegradable poly(lactide-*co*-glycolide) core for the targeted delivery of anticancer drugs. However, a laborious fabrication technique cannot be avoided.

As a means of developing new thermo-responsive stealth PLs bearing nanocarriers, we have designed new biocompatible lipopolymer micelles as delivery vehicles with an active targeting ligand. Poly(*N*-isopropylacrylamide) [p(NIPAM)], a key member of the temperature responsive polymers,[18] has been extensively employed for the synthesis of various single/dual/multi stimuli nanocarriers.[19] Here, alkyne terminated p(NIPAM)$_n$ with different molecular weights (MWs) were prepared by a reversible addition-fragmentation chain transfer (RAFT) polymerization using an alkyne functionalized chain transfer agent (CTA). Three different PLs such as 1,2-dipalmitoyl-*sn*-glycero-3-phosphoethanolamine (DPPE), soybean lecithin based L-α-phosphatidylethanolamine (SPE) and 1,2-bis(10,12-tricosadiynoyl)-*sn*-glycero-3-phosphoethanolamine (DCPE) were then bioconjugated to yield PL-p(NIPAM)$_n$ (n = 25, 40, 60) hybrid materials. Folic acid (FA) was also tethered to improve "active tumor-targeting" ability[20] of the PNCs. The release behavior of doxorubicin (Dox)-encapsulated PNCs fabricated by the self-assembly of the resulting PL-p(NIPAM)$_n$/PL-p(NIPAM)$_n$-FA mixture was evaluated at a range of temperatures. The FA receptor–mediated delivery of the PNCs and the temperature-responsive anticancer effect were also assessed by using KB cell lines.

Experimental

Materials

1-Dodecanethiol (98.5%), tetramethylammonium bromide (98.5%), carbon disulfide (99.9%), 2-amino ethanol (97%), triethylamine (TEA, 99.5%), 4-(dimethylamino)pyridine (DMAP, 99%), 1-ethyl-3-(3-dimethylaminopropyl)carbodiimide (EDC, 99.0%), 2,2′-azobis(2-methylpropionitrile (AIBN, 98%), propargyl alcohol (98%), 5-bromovalerate (97%), bromotris(triphenylphosphine)copper(I) ($Cu(PPh_3)_3Br$), and doxorubicin hydrochloride (Dox) were purchased from Sigma-Aldrich and used without further purification. *N*-Isopropylacrylamide (NIPAM, 97%) from Acros Organics was recrystallized from hexane. *N*,*N*-Dimethylformamide (DMF) and *N*,*N*-dimethyl acetamide (DMAc) were distilled over sodium. Acetone and chloroform were distilled over calcium hydride. DPPE and DCPE were purchased from Avanti Polar Lipids, and SPE was extracted from soybean lecithin by solvent extraction.[21] All the other chemicals were reagent-grade, purchased from Sigma-Aldrich and used without further purification

Instrumentation and measurements

^{1}H NMR (400 MHz), ^{13}C NMR (100 MHz), and ^{31}P NMR (161.9 MHz) spectra were recorded on a Varian INOVA 400 NMR spectrometer. The temperature-dependent ^{1}H NMR measurements were performed after the sample tube was allowed to equilibrate at each preset temperature for approximately 10 min. Chemical shifts are presented in parts per million (ppm) relative to the residual solvent peaks as the internal standard. Peak multiplicities in ^{1}H NMR spectra are abbreviated as s (singlet), d (doublet), t (triplet), m (multiplet), and br (broad). Column chromatography was performed using a Combi-Flash Companion purification systems (Teledyne ISCO) using 300–400 mesh silica gel. UV-vis turbidimetry experiments were carried out for LCST determination on a Shimadzu UV-1650 PC equipped with a temperature controller. Fourier transform infrared (FT-IR) spectra were recorded on a Shimadzu IRprestige 21 spectrometer. The spectra were taken on KBr discs in the range 4000–600 cm^{-1}. The molecular weight and polydispersity index (Đ) of the polymers were measured on a Waters GPC system, which was equipped with a Waters 1515 HPLC solvent pump, a Waters 2414 refractive index detector, and three Waters Styragel High Resolution columns (HR4, HR2, HR1, with effective molecular weight ranges of 5000–500,000, 500–20,000, and 100–5000 g/mol, respectively) at 40 °C using high-performance liquid chromatography (HPLC)-grade tetrahydrofuran (THF) containing 0.1 N LiBr as eluent at a flow rate of 1.0 mL/min. Monodisperse polystyrenes were used to generate the calibration curve.

Dynamic light scattering (DLS) measurements were carried out using a Nano ZS90 zeta potential analyser (Malvern Instruments, Ltd., U.K.) with a He–Ne laser (633 nm), 90° collecting optics, and a thermoelectric Peltier temperature controller. Block copolymer solutions (2 mg/mL) were filtered through a 0.5-μm filter prior to use. Temperature-dependent DLS experiments were performed after equilibrating the samples for 10 min. Particle morphology have analysed by scanning electron microscope (SEM) and transmission electron microscopy (TEM). SEM consist of an optical microscope (Eclipse 80i, Nikon Co., Japan) with 100x and 1000x magnification was equipped with transmittance and reflective modes and used to observe the morphology of the PNCs. Before the analysis, the samples were fixed to copper stubs using carbon adhesive tape and sputter-coated with 10 nm gold particles. TEM was performed using a JEOL–1299EX electron microscope with an accelerating voltage of 80 keV. TEM samples were prepared by the grids with formvar film were treated with oxygen plasma (from a Harrick plasma cleaner/sterilizer) for 15 s to make their surface hydrophilic. A TEM grid was then floated on top of the bead with the hydrophilic face in contact with the solution; the aqueous solution was blotted away with a strip of filter paper and then the samples were dried overnight at room temperature.

Synthesis of *S*-1-dodecyl-*S*-(α,α'-dimethyl-α''-acetic acid) trithiocarbonate CTA (Scheme 1) The synthesis of *S*-1-dodecyl-*S*'-(α,α'-dimethyl-α''-acetic acid) trithiocarbonate chain transfer agent (trithiocarbonate CTA) was carried out according to a previously reported method.[22] In brief, 4.04 g of dodecanethiol (20 mmol), 10 mL of acetone, and 0.26 g of tetrabutyl ammonium bromide (0.8 mmol) were added to a 50-mL flask, and nitrogen gas was bubbled through the solution for 30 min at 10 °C. An aqueous solution of 1.68 g of 50 wt % sodium hydroxide (21 mmol) was subsequently slowly

added at temperature below 10 °C. After stirring for 15 min, a carbon disulfide solution in acetone was added in a drop-wise manner (CS_2: 1.525 g, 20 mmol; acetone: 2.015 g, 34.5 mmol). The system was stirred for another 15 min prior to the addition of 2.4 mL of chloroform (30 mmol) and 8 g of 50 wt % sodium hydroxide (100 mmol) at temperature below 10 °C. The ice bath was removed 30 min later, and the reaction was allowed to proceed for 12 h before the addition of 30 mL of distilled water and 5 mL of hydrochloric acid (6.8 M). After 30 min, the system was distilled under reduced pressure to remove the volatile solvents, resulting in the appearance of a yellow precipitate which was collected by filtration. The precipitate was dissolved in 100 mL of isopropanol under strong stirring, and the undissolved residue was removed by filtration. The filtrate was subsequently distilled under reduced pressure to remove isopropanol, and the remaining residue was recrystallized in hexane and dried in vacuum for one day. At the end, 4.3 g of trithiocarbonate CTA was obtained as pale yellow solid (Yield = 45%). ^{1}H NMR (400 MHz, $CDCl_3$) δ (ppm) = 0.87 (t, 3H, $CH_3C_{10}H_{20}CH_2$–), 1.26–1.71 (m, 20H, $CH_3C_{10}H_{20}CH_2$–), 1.72 (s, 6H,–S(CS)S–C(CH_3)$_2$–COOH), 3.28 (t, 2H, $CH_3C_{10}H_{20}CH_2$–). ^{13}C NMR (100 MH_Z, $CDCl_3$) δ (ppm) = 14.8, 22.8, 23.2, 28.9, 30.0, 30.3, 31.1, 32.5, 34.3, 55.1, 172.5, 220.3.

Synthesis of alkyne-terminated CTA (CTA–alkyne) Alkyne-terminated *S*-1-dodecyl-*S*'-(α,α'-dimethyl-α''-acetic acid) trithiocarbonate was synthesized by esterification of trithiocarbonate CTA using propargyl alcohol. Trithiocarbonate CTA (2 g, 5.5 mmol), EDC-HCl (2.12 g, 11 mmol), and DMAP (0.067 g, 0.55 mmol) were mixed in 20 mL of dry CH_2Cl_2. Propargyl alcohol (0.635 mL, 11 mmol) was added dropwise to the mixture at 0 °C, and the resulting transparent yellow solution was stirred at room temperature for 48 h. The mixture was subsequently washed three times with distilled water. The ester was further purified with silica column chromatography (eluent: a mixture of petroleum ether and ethyl acetate with a volume ratio of 1:1), and the alkyne-terminated CTA was obtained as a pale yellow liquid (Yield = 51%). ^{1}H NMR (400 MHz, $CDCl_3$) δ (ppm) = 0.87 (t, 3H, $CH_3C_{10}H_{20}CH_2$–), 1.26–1.71 (m, 20H, $CH_3C_{10}H_{20}CH_2$–), 1.72 (s, 6H,–S(CS)S–C(CH_3)$_2$–COOH), 3.28 (t, 2H, $CH_3C_{10}H_{20}CH_2$–). ^{13}C NMR (100 MHZ, $CDCl_3$) δ (ppm) = 14.8, 22.8, 23.2, 28.9, 30.0, 30.3, 31.1, 32.5, 36.3, 53.4 56.1, 76.2, 78.3 172.5, 221.2.

RAFT polymerization of NIPAM using CTA–alkyne A Schlenk tube containing a reaction mixture of NIPAM (1.1760 g, 10.4 mmol), CTA-alkyne (66.1 mg, 0.1 mmol), and AIBN (3.344 mg, 0.02 mmol) in DMF (4 mL) was degassed by three freeze–pump–thaw cycles, and the solution was stirred at 70 °C under N_2 for 24 h. Precipitation in ethyl ether twice yielded alkyne-terminated p(NIPAM) [p(NIPAM)-alkyne]$_n$ as a white powder. p(NIPAM)$_n$ (n = 25, 40, 60) ^{1}H NMR (400 MHz, $CDCl_3$) δ (ppm) = 0.98 (t, 3H, $CH_3C_{10}H_{20}CH_2$–), 1.28 (br, CH(CH_3)$_2$, 1.30–1.96 (br, 20H, $CH_3C_{10}H_{20}CH_2$–), 2.52 (br, CH_2), 3.47 (br, CH), 3.94 (br, CH), 4.40 (m, 2H, OCH_2), 6.21 (br, NH). ^{13}C NMR (100 MHz, $CDCl_3$) δ (ppm) = 14.08, 20.9, 21.6 23.1, 23.81, 23.1, 28.9, 30.3, 30.9, 31.7, 32.5, 34.1, 39.4, 40.3,41.3, 45.6, 52.8, 67.5, 174.1, 174.5, 221.7.

Synthesis of azide-functionalized lipids Lipid-NH_3^+ (DPPE, DCPE or SPE) (0.25 mmol) and precursor succinimidyl 5-azidovalerate[23] (0.028 mmol) were dissolved in chloroform (14 mL) in a 100-mL round-bottom flask with a magnetic stirrer. A solution of triethylamine (54 mg, 0.67 mmol) in 2 mL of chloroform was added to the reaction mixture and stirred at 30 °C for 2 h. The reaction mixture was subsequently washed with water (3 × 30 mL). The solvent was removed under reduced pressure and flash column silica gel chromatography was performed using an 80:20 mixture of chloroform: methanol as an eluent for the separation of azide-terminated lipids (DPPE–N_3, DCPE–N_3 and SPE–N_3) with around 65% yields. For DPPE-N_3, MS (fast atom bombardment (FAB), *m/z*) $[M+Na]^+$ calculated for $C_{42}H_{80}N_4O_9P$, 837.57, found 837.6; elemental analysis calculated for $C_{42}H_{80}N_4O_9P$ (%) C=61.81, H=9.88, N=6.87, found C= 60.74, H=9.63 and N=6.19. The azide-functionalized lipids were also characterized by NMR and FT-IR spectroscopies.

Synthesis of lipid–p(NIPAM)$_n$ hybrid by click reaction Following the mixing of 0.08 g (0.1 mmol) of DPPE–N_3 with 10.0 mL of $CHCl_3$, 0.7 g of alkyne-terminated PNIPAM (M_n = 7000, 0.1 mmol) and 0.5 mol% of Cu(PPh_3)$_3$Br were added. The reaction was allowed to proceed for 24 h under inert atmosphere at room temperature. Click reaction of the material was verified by the observation of a complete disappearance of azide stretching in the FT-IR spectrum. The reaction mixture was passed through the silica gel to remove the catalyst and the product precipitated in n-hexane to yield a white powder (DPPE–p(NIPAM)). Click reactions were also performed in similar procedures by using other lipids (SPE–N_3 and DCPE–N_3) and p(NIPAM)s with different MWs. .

Folic acid conjugation by thiol-ene click reaction For the aminolysis of thiocarbonyl moiety,[24] a lipid-conjugated p(NIPAM) was dissolved in chloroform and stirred for 2 h under a nitrogen atmosphere in the presence of 1-hexaneamine and tributylphosphine. The resulting thiol-terminated lipid-p(NIPAM)$_n$–SH was obtained as a white powder after precipitation in cold ether and dry under reduced pressure. The aminolysis was traced by the complete disappearance of RAFT entity at 308 nm by UV-visible spectrophotometer.

The synthesis protocols for allyl folate was derived from previous report[19a] with minor alterations. Folic acid (1 g, 2 mmol) was dissolved in DMF (5 mL) and cooled in an ice bath. *N*-Hydroxysuccinimide (260 mg, 25 mmol) and EDC (440 mg, 25 mmol) were added, and the resulting mixture was stirred in the ice bath for 30 min to yield a white precipitate. A solution of allyl alcohol (124 mg, 2.25 mmol) in DMF (5.0 mL) was added, and the resulting mixture was allowed to warm to room temperature and stirred for 24 h. The reaction mixture was then poured into water (100 mL) and stirred for 30 min to form a precipitate. The orange-yellow precipitate was filtered, washed with acetone, and dried under vacuum for 6 h to yield 83% allyl folate.

For the thiol-ene click reaction allyl folate was dissolved in DMF and DMF-dissolved solution of DPPE–p(NIPAM)$_n$–SH and

TEA was added dropwise. The solution was stirred at room temperature for 12 h under a nitrogen atmosphere. The product was precipitated in ice-cold ether (three times) and folic acid-conjugated lipopolymer was dissolved in DMF and dialyzed for 6 h using a membrane with molecular weight limit of 1000 Da. The folic acid-conjugated lipopolymer (DPPE–p(NIPAM)$_n$–FA) were isolated by lyophilization.

Fabrication of hybrid nanocarriers

Hybrid PNCs were prepared by a combination of self-assembly-derived precipitation and a membrane-dialysis method. DPPE–p(NIPAM)$_n$ (9 mg) and DPPE–p(NIPAM)$_n$–FA (1 mg) was dissolved in DMAc (7 mL) and deionized water (3 mL) was added. The turbid mixture was then dialyzed against deionized water for 2 days using a dialysis membrane (regenerated cellulose) with a 2000 Da molecular weight cut-off (MWCO = 2000) at 20 °C. The outer phase was replaced at 3 h intervals with fresh water. The solution was subsequently lyophilized after filtering through a 0.2-μm syringe filter to remove any impurities and non-liposomal aggregates (yield = 61%). For Dox-loaded PNC, Dox (20 mg) dissolved in DMAc (7 mL) and TEA (1.5 equivalent to Dox) was added to the solution of DPPE–p(NIPAM)$_n$ (18 mg) and DPPE–p(NIPAM)$_n$–FA (2 mg) dissolved in DMAc (14 mL) at room temperature with mixing. Following the addition of 6 mL of water, the resulting drug-loaded PNC solution was dialyzed against deionized water using a dialysis membrane (MWCO = 2000) at 20 °C for 2 d (yield = 58%).

Determination of drug loading content (DLC), drug loading efficiency (DLE)

For the quantification of drug (Dox) encapsulation, aliquots of the drug-loaded PNC solution were lyophilized and broken up by adding 2 mL of DMSO. The obtained solution was analyzed using UV–Vis spectroscopy. The characteristic absorbance of Dox (485 nm) was recorded and compared with a standard curve generated in DMF with drug concentrations ranging from 0 to 100 mg/mL. The percentages of DLC and DLE were calculated using the following equations (1) and (2):

DLC (%) = (weight of Dox in PNCs/weight of Dox-loaded PNCs) × 100 (1)

DLE (%) = (weight of Dox in PNCs /weight of Dox for Dox-loaded PNCs preparation) × 100 (2)

***In vitro* intrinsic cytotoxicity of PNCs**

To assess the intrinsic cytotoxicity of the PNC fabricated by DPPE–p(NIPAM)$_n$ (n = 25, 40, 60) and DPPE–p(NIPAM)$_n$–FA mixture human KB carcinoma cells were seeded in 96-well plates and incubated overnight at 5% CO_2 and 37 °C. Cells were treated with empty PNCs in serum-free RPMI 1640 media for 24 h. Viability of cells was assessed following treatment using the 4,5-dimethylthiazol-2-yl)-2,5-diphenyltetrazolium bromide (MTT) viability test. MTT (25 × l; 2 mg/mL) was added to each well of the 48-well plates and the mixtures incubated for 4 h. The formazan crystals formed in living cells were solubilized with a sodium dodecyl sulfate (SDS)/HCl solution (SDS, 10% w/v; HCl 0.1 N). The absorbance was determined at 570 nm using an automated computer-linked microplate reader (Molecular Devices, Sunnyvale, CA, USA).

Receptor-mediated delivery of hybrid PNCs

Folic acid receptor-mediated delivery of PNC was assessed using KB cells. KB cells were seeded onto cover-glass in 6-well plates. Cells were cultured overnight in RPMI 1640 media (supplemented with 10% fetal bovine serum (FBS) and 1% antibiotics) in an incubator at 5% CO_2 and 37 °C. Cells were pretreated with folic acid (2 mM) 1 h prior to treatment with Dox or PNC to block the folic acid receptors (FA (+)). Following pre-treatment, cells were exposed to Dox or PNC (Dox concentration was equivalent to 5 μg/mL) for 1 h. FA (-) cells were treated with Dox or PNC at identical concentrations without pre-treatment with folic acid. For PNC treatments, lyophilized PNCs were carefully reconstituted into folic acid-free RPMI 1640 medium. To study thermosensitive drug delivery, 6-well plates were incubated at a range of temperatures (4, 20, and 37 °C). Cells were subsequently washed with PBS and fixed with 4% paraformaldehyde. Cells were mounted with immobilization solution (ImmuMount, Thermo Electron Corporation, Pittsburgh, PA, USA) and observed with confocal laser scanning microscopy (TCS-SP2 microscope, Leica, Wetzlar, Germany).

For flow cytometric analysis of receptor-mediated delivery of PNC, 1 × 10^6 KB cells were seeded in 6-well plates and cultured overnight in an incubator at 5% CO_2 atmosphere. Dox or PNC treatments were performed as described above. To block folic acid receptors, cells were incubated with 2 mM folic acid 1 h before treatment with Dox or PNC. To study thermosensitive drug delivery, 6-well plates were incubated at a range of temperatures (4, 20, and 37 °C). Following 1 h incubation, cells were harvested and analysed with a flow cytometer. A 488 nm excitation wavelength and 522 nm emission wavelength were used to observe the fluorescence intensity of Dox. Folic acid-free RPMI 1640 medium was used in all procedures of the cell culture experiments.

***In vitro* anticancer activity**

Anticancer activity of Dox-loaded hybrid mycelle against KB cells (squamous carcinoma) was estimated using the MTT viability assay. KB cells (1 × 10^5) were seeded in 48-well plates and incubated overnight in an incubator at 5% CO_2. To block folic acid receptors, cells were incubated with 2 mM folic acid (FA (+)) for 1 h before the addition of hybrid PNC. Following incubation, cells were exposed to Dox or PNC in folic acid-free RPMI 1640 medium (FA (-)) in each well of the 48-well plates for 12 h before the medium was replaced with serum-free RPMI 1640. Cells were cultured for 1 day prior to the addition of 50 × l MTT (2 mg/mL) to each well of the 48-well plates and subsequent 1 h incubation. The formazan crystals formed in living cells were solubilized with SDS/HCl solution (SDS, 10% w/v; HCl 0.1 N). The absorbance was determined at 570 nm using an automated computer-linked microplate reader (Molecular Devices).

Results and discussion

Synthesis of alkyne-terminated p(NIPAM)$_n$ and azide terminated PLs Alkyne-terminated p(NIPAM)$_n$ (n = 25, 40, 60) with different MWs was synthesized by using the RAFT polymerization of alkyne-terminated CTA. As summarized in Scheme 1, the alkyne-terminated thiocarbonate CTA was prepared using a previously reported procedure.[22] The alkyne functionality of CTA was confirmed by the chemical shifts at 4.66 and 2.45 ppm from the ^{1}H NMR spectrum and the chemical shift at 73 and 76 ppm from the ^{13}C NMR spectrum (Figure S1 in the Supporting Information (SI)). FT-IR spectrum also displayed the terminal alkyne functionality by alkyne stretching at 3325 cm^{-1}. The RAFT polymerization of NIPAM using the resulting CTA yielded well-defined alkyne-terminated p(NIPAM)$_n$ (n = 25, 40, 60) (Table 1; Figure S2 of SI). The Đ value of polymers was observed in the range between 1.10 and 1.28.

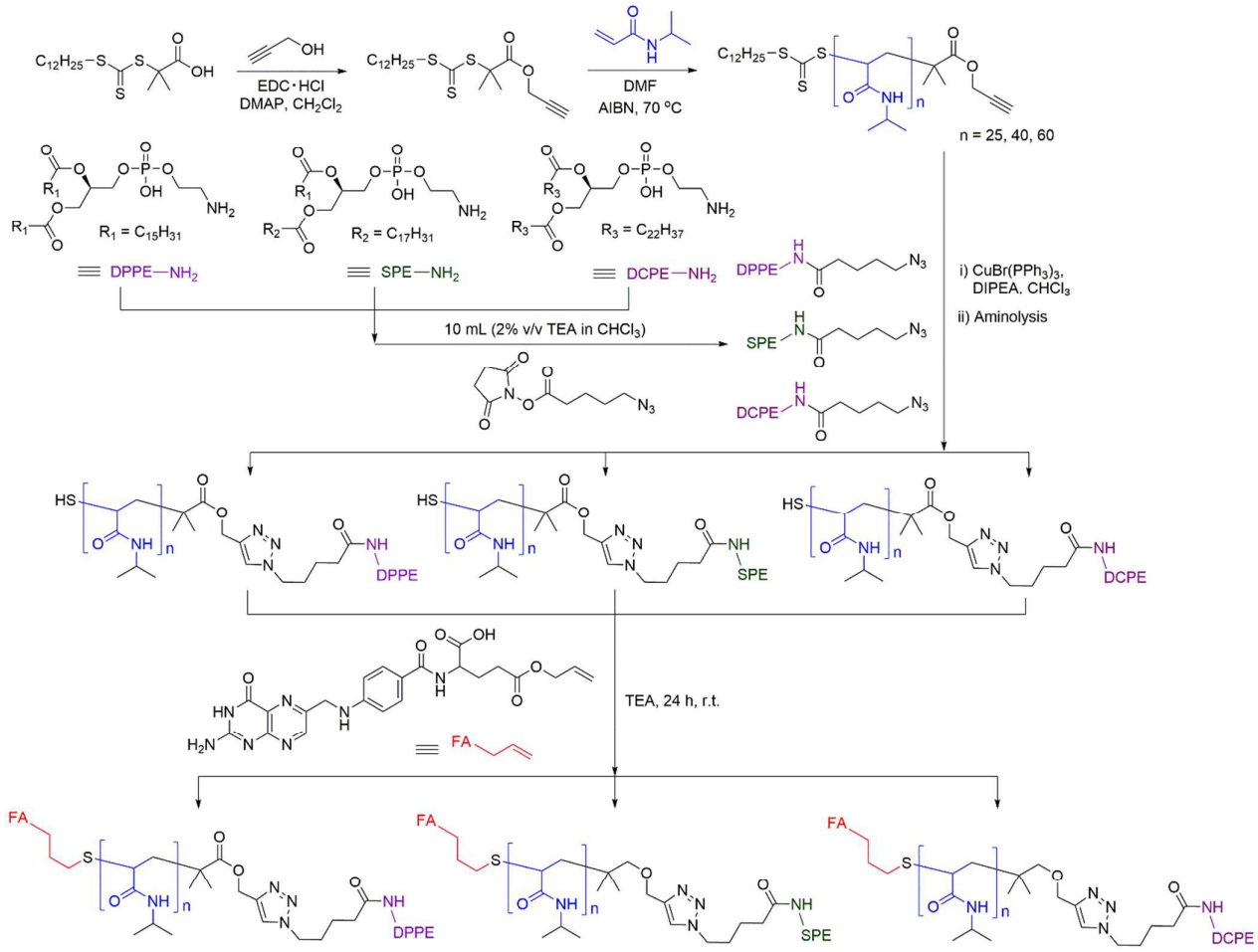

Scheme 1. Synthesis of folic acid-tethered phospholipid–p(NIPAM)$_n$ (n=25, 40, 60) bioconjugates by combining RAFT polymerization with a series of click reactions.

Table 1. Characterization of alkyne-terminated p(NIPAM) obtained by RAFT polymerization.

Theor. Comp.	Yield (%)	M_n (g/mol) Theor.[a]	NMR	GPC	Đ[b]
p(NIPAM)$_{25}$	59	2800	2700	3100	1.14
p(NIPAM)$_{40}$	64	4400	4200	5300	1.16
p(NIPAM)$_{60}$	65	6700	6500	7600	1.28

[a]Theoretical number-average molecular weights calculated using the equation: $M_{n,theor.} = M_M \times conv. \times [M]_0/[CTA]_0 + M_{CTA}$ where M_M is the MW of the monomer; conv. is the monomer conversion as determined by ^{1}H NMR spectroscopy; $[M]_0$ and $[CTA]_0$ are initial concentrations of the monomer and CTA, respectively; and M_{CTA} is the MW of CTA. [b]Polydispersity index measured by GPC.

For the synthesis of azide-functionalized PLs, PLs–NH_2 react with succinidimyl 5-azidovalerate in the presence of TEA. Major part of the side product is *N*-Hydroxysuccinamide and triethyl ammonium ion were removed by aqueous wash. For the further purification of PL–N_3 was performed by column chromatography in chloroform: methanol (8:2) as an eluent. The azide functionalization of PLs was confirmed by the spectroscopic analyses (see FT-IR spectra (Figure S3), ^{1}H-(Figure S4) and ^{13}C-NMR (Figure S5) spectra in SI). FT-IR spectra

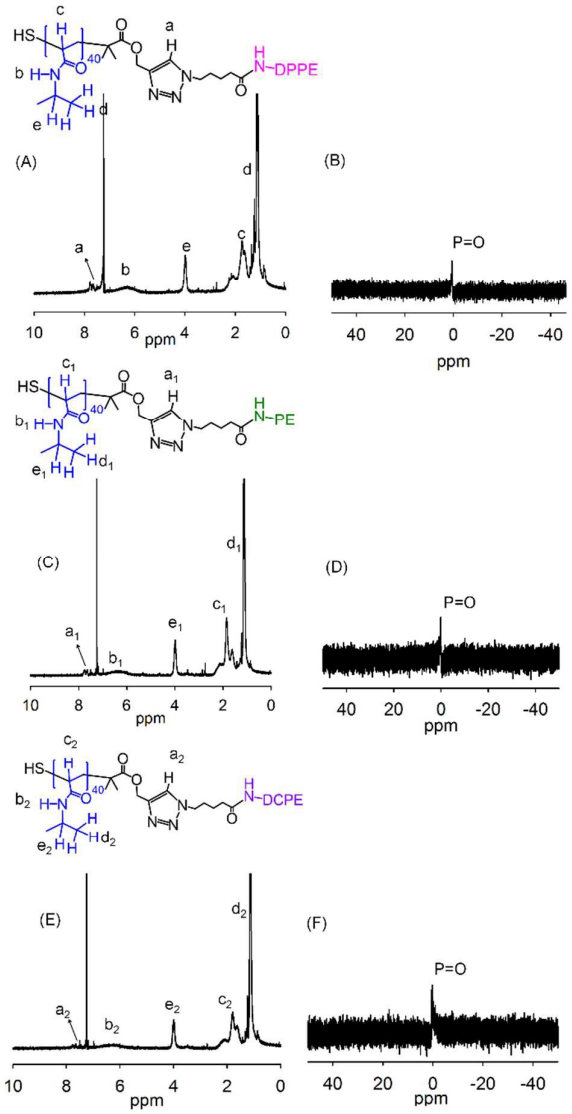

clearly show azide stretching of PLs–N_3 at 2230 cm^{-1}. Additionally, Figure S5 shows the chemical shift at δ = 50 ppm, assigned to the methylene carbon (-CH_2-N_3) bonded to azide groups.

Figure 1. ^{1}H (A, C, E) and ^{31}P (B, D, F) NMR spectra of thiol-terminated PL–p(NIPAM)$_{40}$ hybrids.

Synthesis of thiol-terminated PL–p(NIPAM)$_n$–SH and folic acid-tethered PL–p(NIPAM)$_n$–FA bioconjugates For the bioconjugation of PLs onto alkyne-terminated p(NIPAM)$_n$,

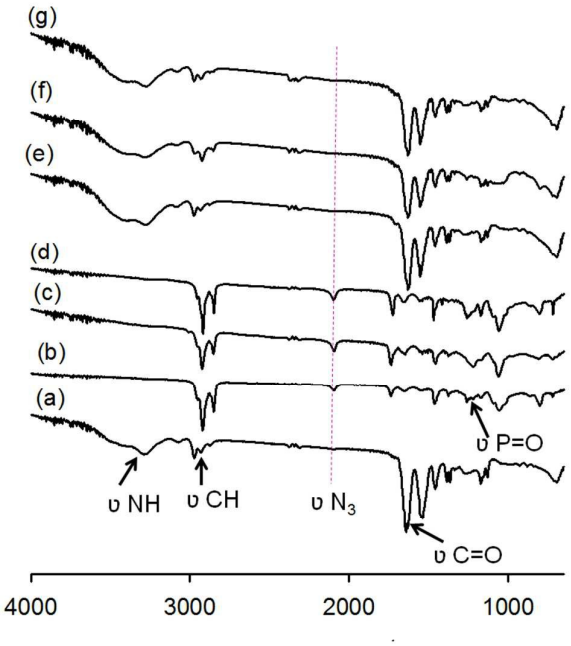

amine moieties of PL were converted to azide groups to yield PLs–N_3, and then azide-alkyne click reactions were performed. The pure lipopolymers, DPPE–p(NIPAM)$_n$, DCPE–p(NIPAM)$_n$ and SPE–p(NIPAM)$_n$, were obtained after the removal of the catalyst and the removal of the thiocarbonyl moieties in lipopolymer hybrids by aminolysis.[24]

Figure 2. FT-IR spectra of alkyne-terminated p(NIPAM)$_{40}$ (a); azide-functionalized PLs, DPPE–N_3 (b), SPE–N_3 (c) and DCPE–N_3 (d); PL–p(NIPAM)$_{40}$ hybrids after the click reaction followed by aminolysis, DPPE–p(NIPAM)$_{40}$ (e), SPE–p(NIPAM)$_{40}$ (f) and DCPE–p(NIPAM)$_{40}$.

The structures of thiol-terminated DPPE–p(NIPAM), SPE–p(NIPAM) and DCPE–p(NIPAM) obtained by alkyne-azide click reactionwere characterized using NMR and FTIR spectroscopies. Figure 1 shows ^{1}H and ^{31}P NMR spectra of PL–p(NIPAM)$_{40}$ as representative samples. The presence of =CH– protons in the triazole ring and the merged peak of –NH– protons in the lipid moieties with the those in NIPAM repeating units, a broad peak at δ = 6.2–7.02 ppm, demonstrate the successful click reaction. Additionally, the ^{31}P NMR spectra of PLs–p(NIPAM)$_{40}$ show a chemical shift at δ = -1.3 ppm, confirming the successful conjugation. Hay *et al.*[25] reported a strong isotropic resonance at -1.33 ppm in the ^{31}P NMR of p(NIPAM)–dimyristoylphosphatidylethanolamine conjugate obtained by carmodiimide coupling strategy. The click reaction was also identified by the disappearance of azide stretching vibration of PL–N_3 at 2230 cm^{-1} in the FTIR spectrum of PLs–p(NIPAM)$_{40}$ (Figure 2).

The end-group removal is an important issue for RAFT-CTA functionality in polymer materials, because they may

decompose to produce malodorous sulfur-containing materials.[26] We have successfully removed the thiocarbonyl moieties by aminolysis to transform the thiocarbonyl-containing groups into thiol groups, which can be used for further coupling. The removal of thiocarbonyl moieties was confirmed by comparing the UV-visible spectra of CTA, alkyne-terminated p(NIPAM)$_{25}$–CTA, PLs–p(NIPAM)$_{25}$–CTA and PLs–p(NIPAM)$_{25}$–SH (Figure S6). The absorbance of at 308 nm assigned to RAFT entity is completely disappeared by aminolysis. The resulting ω-functional thiol groups are to be used for thiol-ene click reaction to conjugate folate for active targeting of cancer cells (*vide infra*).

For the thiol-ene click reaction of PLs–p(NIPAM)$_n$–SH with folate moiety, we have synthesized an allyl-terminated folic acid by the esterification of folic acid with allyl alcohol in the presence of EDC and DMAP. The reaction mixtures were poured into water and an orange-yellow precipitate was filtered and dried under reduced pressure. Figure S7 shows the ^{1}H NMR spectra of the allyl-folate. The chemical shifts at 5.29 and 5.67 ppm confirm the successful esterification. The click reactions of allyl-folate with thiol-terminated PLs–p(NIPAM)$_n$–SH were performed according to Scheme 1. Figure 3 shows ^{1}H NMR spectrum of folic acid-tethered DPPE–p(NIPAM)$_{40}$–FA as a representative example. The chemical shift at δ = 8.67 ppm shows the presence of pteridine ring of the allyl-folate in the DPPE–p(NIPAM)$_{40}$–FA polymer hybrids, according to previous reports by Sumerlin and co-workers.[19a] Additionally, when spectra are compared with Figure S7, the allyl proton of allyl-folic acid at δ = 5.29 and 5.64 ppm (–C<u>H</u>=C<u>H$_2$</u>) disappeared after the thiol-ene reaction and the protons near δ = 6–7.5 ppm of folic acid merged with the –NH– proton of the p(NIPAM)$_{40}$ repeating units. The spectroscopic data reveal the successful conjugation of the folic acid ligand to the lipopolymer hybrids. Their ability to target drug delivery has been subsequently proven by the receptor-mediated delivery of Dox described in the following sessions.

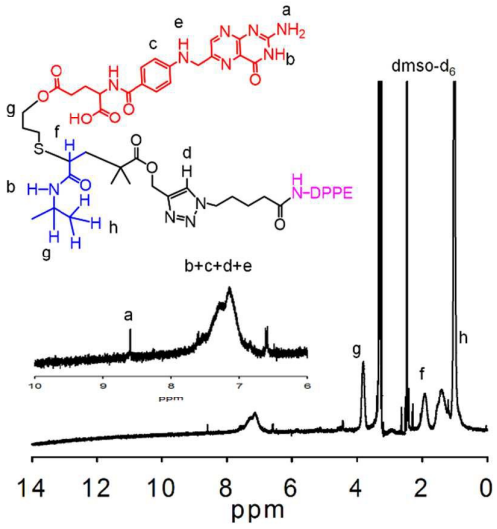

Figure 3. ^{1}H NMR spectrum of folic acid-conjugated DPPE–p(NIPAM)$_{40}$–FA.

Temperature-responsive phase transition behaviour of PL–p(NIPAM)$_n$ hybrids Several studies have described broad structural variations in the p(NIPAM)$_n$ block with the incorporation of the hydrophobic graft or blocks used for temperature-regulated release of the entrapped dye or therapeutic agents. These findings suggest a reversible thermo-responsiveness around the lower critical solution temperature (LCST) due to the transition of the p(NIPAM) chain from coil to globule resulting from the aggregation of dehydrated macromolecules.[18] In our study, PLs-p(NIPAM)$_n$ showed a similar thermos-responsive behaviour as the p(NIPAM)$_n$ homopolymer at temperatures above LCST, with respective changes caused by the incorporation of lipid as a hydrophobic unit. The thermally responsive aggregation behavior of PLs-p(NIPAM)$_n$ was confirmed by ^{1}H NMR spectroscopy with a polymer concentration of 70 mg/mL in D_2O. The temperature-dependent ^{1}H NMR spectra of lipid-p(NIPAM)$_n$ are shown in Figure S8, presenting the spectra of (a) DPPE–p(NIPAM)$_{40}$, (b) SPE–p(NIPAM)$_{40}$, and (c) DCPE–p(NIPAM)$_{40}$, as the representative of each lipopolymer family series. The ^{1}H NMR spectra of PL–p(NIPAM)$_{40}$ suggested a reversible appearance and disappearance of p(NIPAM) peaks in solution between 27 and 50 °C. Additionally, PLs-induced signals were unchanged or shifted at higher temperatures, but the signal corresponding to p(NIPAM) decreased at temperatures above 32 °C and completely disappeared at 41 °C. Therefore, our PLs-conjugated compound exhibited the coil-to-globule transition at temperatures near the LCST.

The coil-to-globule transitions of p(NIPAM)$_n$ homopolymer and PL–p(NIPAM)$_{40}$ hybrids were examined by turbidimetry measurements using a UV-vis spectrometer. The turbidimetry measurements of lipopolymer hybrids at various temperatures are presented in Figure 4. Here, three series of aqueous solutions of PL–p(NIPAM)$_n$–FA hybrids, DPPE–p(NIPAM)$_n$–FA, SPE–p(NIPAM)$_n$–FA and DCPE–p(NIPAM)$_n$–FA (n = 24, 40, 60), were evaluated by turbidimetric measurements using a UV-vis spectrometer at the concentration of 2.0 mg/mL. We did not observe any significant changes with higher MW p(NIPAM) in the phase transitions above or below LCST. Additionally, we detected no major variation in the LCST measured in the lipids tested, and we observed that the LCST of the lipid-p(NIPAM)$_n$ hybrid is between 36.5 and 37.6 °C, which is close to body temperature (37.2 °C).

Dynamic light scattering measurements There are two classes of p(NIPAM)$_n$–comprising materials, incorporating block copolymers or hybrid materials. The PNCs fabricated below LCST by using the materials bearing a hydrophobic block coupled with p(NIPAM)$_n$ show hydrophobic behaviour above LCST due to the reversible thermal transition of p(NIPAM) units. For instance, Qin et al reported the synthesis of PEG–*b*–p(NIPAM)$_n$ copolymers ($Đ \leq 1.2$) using RAFT polymerization and demonstrated the potential for using the temperature phase transition for therapeutic applications.[27] Recently, Lodge and coworkers have analyzed the phase transition and micellar aggregation behavior of p(NIPAM)$_n$-comprising triblock polymers at temperatures above the LCST using DLS and cryoTEM in aqueous solutions, demonstrating that a

hydrophobic component can tune the LCST of the p(NIPAM) at temperatures above LCST and, at higher p(NIPAM) concentrations, lead to the formation of a hydrogel.[28]

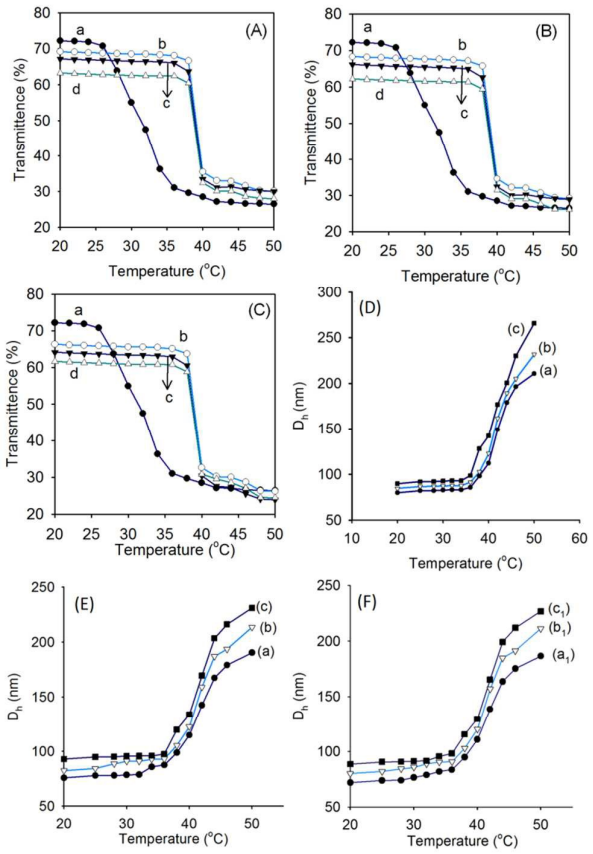

Figure 4. Transmittance versus temperature (A–C) and hydrodynamic diameter (D_h) versus temperature (D–F) curves for aqueous solution (pH 7.4) of PL–p(NIPAM)$_n$–FA hybrids: (A) DPPE–p(NIPAM)$_n$–FA [n = 25 (b), n = 40 (c), and n = 60 (d)]; (B) SPE–p(NIPAM)$_n$–FA [n = 25 (b), n = 40 (c), and n = 60 (d)]; (C) DCPE–p(NIPAM)$_n$–FA [n = 25 (b), n = 40 (c), and n = 60 (d)]; (D) DPPE–p(NIPAM)$_n$–FA [n = 25 (a), n = 40 (b), and n = 60 (c)]; (E) SPE–p(NIPAM)$_n$–FA [n = 25 (a), n = 40 (b), and n = 60 (c)]; and (F) DCPE–p(NIPAM)$_n$–FA [n = 25 (a_1), n = 40 (b_1), and n = 60 (c_1)]. In (A–C) the curves (a)'s correspond to p(NIPAM)$_n$ homopolymers with n = 25, 40 and 60, respectively. Polymer concentration is fixed to 2.0 mg/mL in all experiments.

Additionally, another type of PNC that can form the hydrophobic core and hydrophilic p(NIPAM) corona was evaluated, with the hydrophilic p(NIPAM) corona shown to become hydrophobic because of micellar aggregation at temperatures above LCST. In our current study, we effectively used RAFT for the synthesis of p(NIPAM)s with low *Đ* and used them to conjugate with PLs and further with folate moiety by click reactions. The resulting PL–p(NIPAM)$_n$–FA hybrids were subjected to dynamic light scattering measurements in aqueous solutions at pH 7.4 (Figure 4 (D–F)). At T < 30 °C, the lipid hybrids were dissolved to give hydrodynamic diameter much less than 100 nm, with very weak intensity. Increasing the temperature of the solution increase the size of the aggregation. All series of PL–p(NIPAM)$_n$–FA hybrids show a clear phase transition between 37 and 40 °C. The size of the PNCs increases up to bigger than 200 nm (Figure 4 D-F) at temperatures above 40 °C and finally leads to aggregation at 50 °C. As the chain length of p(NIPAM) increases, the size of the aggregates increases monotonously. In all cases no conspicuous variations in size were observed at temperatures above LCST with respect to various hydrophobic lipid regions in the lipopolymer family.

Fabrication of hybrid PNCs by self-assembly Temperature-responsive lipopolymer hybrid PNCs were prepared by a solvent-exchange method. DPPE–p(NIPAM)$_n$ (n = 25, 40, 60)/DPPE–p(NIPAM)$_n$–FA hybrids were chosen for the self-assemblies. After dissolving 10 mg of lipopolymer hybrid (DPPE–p(NIPAM)$_n$/DPPE–p(NIPAM)$_n$–FA = 9/1 w/w) in 7 mL of DMAc, deionized water was added slowly to the polymer solution. The resulting turbid solution was dialyzed against water to remove the organic solvent at 20 °C. TEM and SEM images of PNCs are shown in Figure 5, revealing that uniform and spherical PNCs are formed by the self-assembly of DPPE–p(NIPAM)$_n$/DPPE–p(NIPAM)$_n$–FA mixtures. As shown in Table 2, the average diameter of the PNCs was approximately 150 nm in diameter. We couldn't observe any remarkable difference in the size of the PNC with increasing length of p(NIPAM) chains. The overall size of the nanocarrier-based drugs is an essential physical aspect that determines the clinical successes, since pathological tissues, such as inflammatory or solid tumor tissues, are characterized by increased vascular permeability.[29] Through the enhanced permeation and retention (EPR) effect characterizing malignant tissues nanocarriers of an appropriate size can pass through tumor-vessel walls and enter the neoplastic lesion. It has been known that nanocarriers smaller than 100 nm in diameter interact less with plasma proteins, evade capture by the reticuloendothelial system (RES), have a longer half-life in the blood, and accumulate passively at the tumoral site.[30] Nanocarriers with too large size are eliminated more rapidly from blood circulation and cannot avoid RES uptake. Considering, at the tissue level, many nanocarrier products including liposomal medicine attempt to target sites passively through the EPR effect, with feature sizes typically in the 100–200 nm range,[5] the size of liposomal products achieved in this study seems to be in an ideal range.

Considering the structure of lipopolymers and the self-assembly procedure adopted in this study, the self-assembled nanocarriers are much like hybrid micelles, with the lipid monolayer hydrophobic core and the hydrophilic p(NIPAM) blocks populating the surfaces corona (Figure 5(g)). The PL monolayer containing hybrid micelles is quite different from liposomes.[31] Note that we name the resulting hybrid micelles as PNCs throughout this paper. Thus, the steric hindrance provided by the lipopolymers minimizes the space available for the encapsulation of drugs and biomolecules. In order to investigate the DLE, similar self-assembly procedure was

performed in the presence of Dox, a hydrophobic anticancer drug widely used in clinical trials. The DLC and DLE data of Dox-

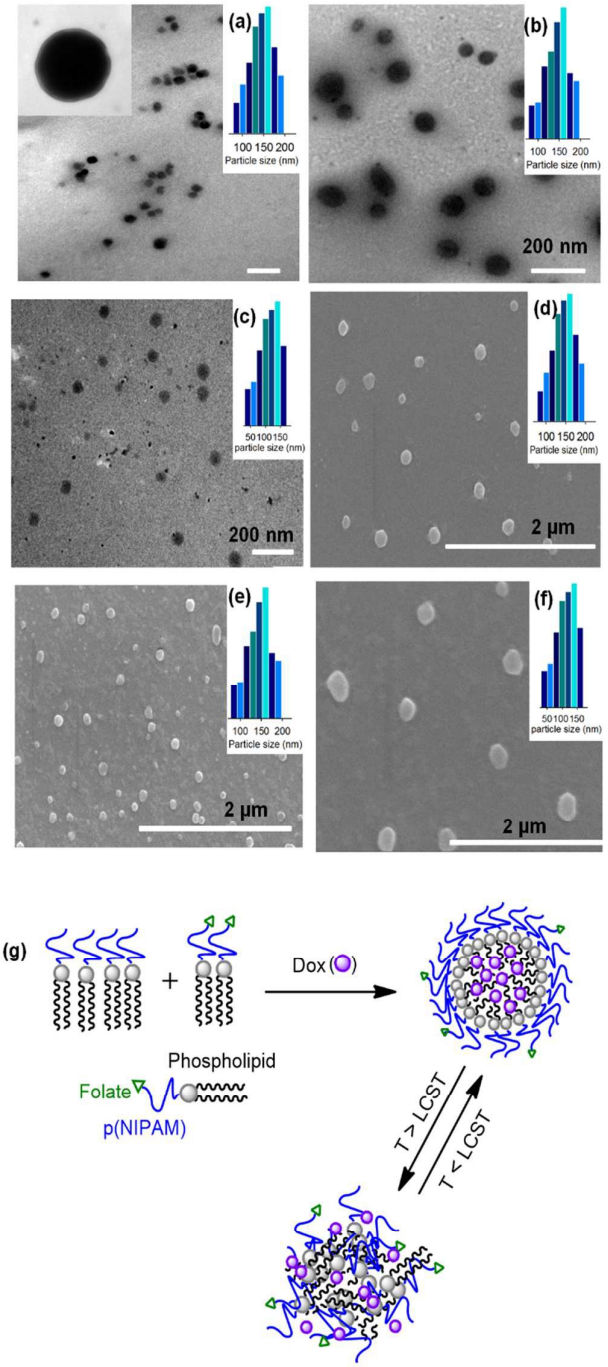

encapsulating PNCs are summarized in Table 2. No significant variations in DLE and DLC according to MW of NIPAM block in Dox-loaded PNCs fabricated by DPPE–p(NIPAM)$_n$/DPPE–p(NIPAM)$_n$–FA mixture in the presence of Dox are observed, and the DLE values are around 40%.

Figure 5. TEM (a–c) and SEM (d–f) images of PNCs fabricated by DPPE–p(NIPAM)$_{60}$/DPPE–p(NIPAM)$_{60}$–FA (a, d); DPPE–p(NIPAM)$_{40}$/DPPE–p(NIPAM)$_{40}$–FA (b, e); and DPPE–p(NIPAM)$_{25}$/DPPE–p(NIPAM)$_{25}$–FA (c, f) mixtures. (g) shows a schematic procedure of PNC formation and a phase transformation of the PNCs at above and below LCST.

Table 2. Average diameters of PNCs fabricated by DPPE–p(NIPAM)$_n$/DPPE–p(NIPAM)$_n$–FA mixtures and the drug-loading content (DLC) and drug-loading efficiency (DLE)

Sample	D_{avg} [a]	DLC (%)	DLE (%)
DPPE-p(NIPAM)$_{25}$–FA	150.1±0.9	10.8	36
DPPE-p(NIPAM)$_{40}$–FA	168.9±1.4	11.4	39
DPPE-p(NIPAM)$_{60}$–FA	176.1±2.1	11.9	43

[a] Average diameter determined by DLS.

Cytotoxicity of lipopolymer hybrids Intrinsic cytotoxicity of polymers was evaluated using empty PNCs prepared by DPPE–p(NIPAM)$_n$/DPPE–p(NIPAM)$_n$–FA mixtures with results presented in Figure 6(a). All the PNCs exhibit negligible intrinsic cytotoxicity against KB cells, with cell viability maintained above 80% relative to controls at incubations with 100 μg/mL. These results indicate that polymers themselves have very little intrinsic cytotoxicity.

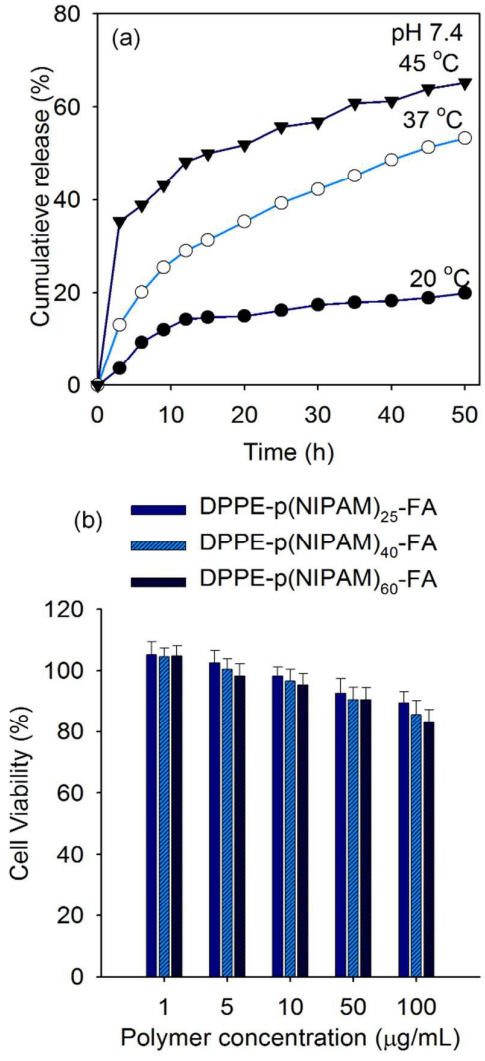

Figure 6. Cytotoxicity (a) of PNCs at a range of concentrations assessed in KB cells and time-dependent release (b) of Dox from the PNCs fabricated by DPPE–p(NIPAM)$_{60}$/DPPE–p(NIPAM)$_{60}$–FA mixture.

Stimuli-responsive release of Dox The aforementioned phase transition of p(NIPAM) at temperatures above LCST induces a complete disassembly of the PNC relative to the hydrophilic units. The time-dependent release of Dox was examined by dialysis method in the phosphate buffered saline (PBS, 7.4) at a range of temperatures, with PNCs fabricated by DPPE–p(NIPAM)$_{60}$/DPPE–p(NIPAM)$_{60}$–FA selected as a representative sample. Dox release was evaluated by measuring the absorbance of the Dox peak at 485 nm in a sample of external PBS solution at different time intervals up to 50 h (Figure 6(b)). The release of encapsulated Dox from the PNCs was particularly enhanced at 37 °C, which is optimal since it facilitates drug release at physiological conditions. These results reveal a temperature responsiveness of the PNCs due to the phase transition of the hydrophilic corona of p(NIPAM)$_{60}$ at temperatures above LCST (Figure 5g). The hydrophobic behaviour of the p(NIPAM)$_{60}$ block was increased due to its poor solubility at temperatures above LCST. Undoubtedly the coil-to-globule phase transition of the p(NIPAM) block affected the nanostructure, allowing the controlled release of Dox at temperatures near the transition temperature range.

Cellular uptake and Dox-loaded delivery of receptor-mediated lipopolymer hybrids Folic acid receptor-mediated and temperature-sensitive delivery of PNCs was studied with squamous carcinoma KB cells over-expressing folic acid receptors. Following pre-treatment of KB cells with folic acid to block the folic acid receptors, cells were exposed to Dox-loaded PNCs as shown in Figure 7, Figures S9 and S10 (optical, fluorescence and merged images). KB cells expressed high intensity of red fluorescence following treatment with all series of polymers at 37 °C. However, fluorescence intensity was significantly decreased when folic acid receptors were blocked by pre-treatment with folic acid. These results indicate that PNCs have the capability of folic acid-receptor mediated delivery. Furthermore, fluorescence intensity was significantly decreased at culture temperatures of 20 and 4 °C with all series of polymers, suggesting that the PNCs are also capable of thermos-sensitive drug delivery.

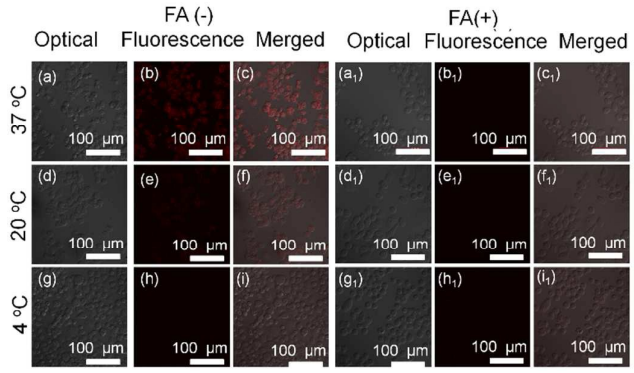

Figure 7. CLSM images of KB cells following incubation with Dox-loaded PNCs of DPPE–p(NIPAM)$_{60}$/DPPE–p(NIPAM)$_{60}$–FA mixture: images of FA (-) and FA (+) cells incubated at 37 °C, 20 °C and 4 °C.

Flow cytometric analysis supported these results, with fluorescence intensity significantly decreased by blocking the folic acid receptors, as shown in Figure 8. The florescence intensity of the Dox-loaded PNCs is enhanced FA non treated KB cells especially at 37 °C (Figure 8 (a)). Temperature responsive Dox PNCs release the Dox at physiological condition on the FA receptor containing cancer cells. In effect, fluorescence intensity observed at 4 °C was similar both in the presence and in the absence of blocking of folic acid receptor and the results are consistent with previous reports. These results indicate that PNCs exhibit sensitivity to both folic acid receptors and temperature.

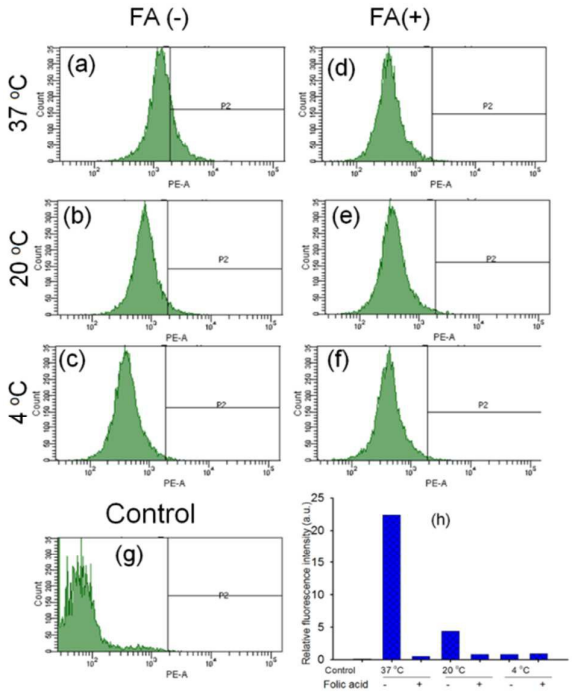

Figure 8. Flow cytometric analysis of KB cells after the receptor mediated accumulation of Dox-loaded PNCs of DPPE–p(NIPAM)$_{60}$/DPPE–p(NIPAM)$_{60}$–FA mixture with FA (-) cells (a–c) and FA (+) cells (d–f) at 4, 20, and 37 °C. The control experiment (independent analysis was done in serum free RpMI1640 media) is presented in (g) and (h). 1.0 ×10^6 cells were used for FACS scan analysis.

Anticancer activity of PNCs was assessed by blocking the folic acid receptors. As shown in Figure 9(a), cell viability gradually decreased with increasing concentrations of Dox and viability following Dox treatment was not significantly altered by the blocking of folic acid receptors. However, cell viability of PNC treatment was increased by blocking the folic acid receptors, as shown in Figure 9(b). These results indicate that PNCs are capable of folic acid receptor-mediated drug targeting and anticancer cancer activity. The new PNCs

fabricated by PL–p(NIPAM)$_n$/PL–p(NIPAM)$_n$–FA mixtures showing both temperature responsiveness and targetablity can be reasonable candidates for smart polymeric delivery vehicle, solving various problems pure PL-based and conventional PEGylated liposomes show.

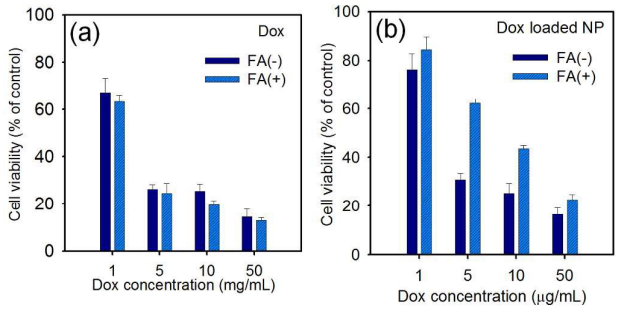

Figure 9. Anticancer activity of free Dox (a) and Dox-loaded PNCs of DPPE–p(NIPAM)$_{60}$/DPPE–p(NIPAM)$_{60}$–FA mixture (b) at a range of concentrations in KB carcinoma cells with folic acid (FA (+)) and without folic acid (FA (-)) pretreatment, assessed at 37 °C.

Conclusions

A series of phospholipids–p(NIPAM)$_n$ bioconjugates, DPPE–p(NIPAM)$_n$, SPE–p(NIPAM)$_n$ and DCPE–p(NIPAM)$_n$ (n = 25, 40, 60), were synthesized by combining RAFT polymerization with azide-alkyne click reaction. The ω-functional thiol group obtained by the aminolysis of thiocarbonyl moieties was further utilized to tether folate by thiol-ene click reaction. According to the characterizations of temperature-responsiveness of the resulting PL–p(NIPAM)$_n$ hybrids using UV-visible and ^{1}H NMR spectroscopies and DLS experiments all the hybrids showed clear phase transitions between 34 and 39 °C. The self-assembly of DPPE–p(NIPAM)$_n$/DPPE–p(NIPAM)$_n$–FA mixtures using a simple solvent-exchange method yielded uniform PNCs with the average size of approximately 150 nm in diameter that is suitable size to passively target sites through the EPR effect. Although the lipid monolayer micelles obtained in this study were much like filled micelles rather than liposomes, the micelles shows reasonable Dox loading efficiency (~40%) and low in time-dependent release tests. The receptor-mediated delivery and release of Dox at 37 °C was assessed in FA(+) and FA(-) cells. The confocal and flow cytometry results were used to monitor cell-specific Dox release. Enhanced anticancer activity was observed at 37 °C with the Dox-encapsulated PNCs of DPPE–p(NIPAM)$_{60}$/DPPE–p(NIPAM)$_{60}$–FA mixture. The results reveal that the hybrid PNCs have potential for use as a drug delivery vehicle and folic acid ligand facilitates specific targeting to cancer tissue and subsequent internalization by endocytosis.

Acknowledgements

This work was supported by the Basic Science Research Program (2012R1A1A2041315) and the Fusion Research Program for Green Technologies (2012M3C1A1054502) through the National Research Foundation of Korea, funded by the Ministry of Science, ICT and Future Planning. The authors also thank the BK21 PLUS Program and Korea Health care Technology R&D project from the Ministry for Health, Welfare and Family Affairs (A091047) for partial financial support.

Notes and references

† Electronic Supplementary Information (ESI) available. See DOI: 10.1039/x0xx00000x

1 T. M. Allen and P. R. Cullis, *Science*, 2004, **303**, 1818-1822.
2 Y. Zhong, F. Meng, C. Deng and Z. Zhong, *Biomacromolecules,* 2014, **15**, 1955–1969.
3 S. Mura, J. Nicolas and P. Couvreur, *Nature materials*, 2013, **12**, 991-1003.
4 J. V. John, R. P. Johnson, M. S. Heo, B. K. Moon, S. J. Byeon and I. Kim, *J. Biomed Nanotechnol.,* 2015, **11**, 1-39.
5 T. Nakaya and Y. J. Li, *Prog. Polym. Sci.* 1999, **24**, 143−181.
6 M. Sophie, C. Benjamin, G. Alain and R. Jean-Jacques, *Biomacromolecules*, 2011, **12**, 1973–1982.
7 C. Xiangji, S. P. Sangram, H. Elizabeth, S. Sallie and E. Todd, *Bioconjugate Chem.,* 2012, **23**, 1753−1763.
8 W. Zhigao, W. Pengjun, D. Mingming, Y. Xuan, L. Jiehua, F. Qiang and T. Hong, *J. Polym. Sci. A Polym. Chem.,* 2011, **49**, 2033–2042.
9 R. P. Johnson, Y. -I. Jeong , J. V. John , C. -W. Chung , S. H. Choi , S. Y. Song , D. H. Kang, H. Suh and I. Kim, *Macromol. Rapid Commun.*, 2014, **35**, 888−894.
10 A. D. Bangham, *J. Mol. Biol.*, 1965, **13**, 238–252.
11 M. L. Immordino, F. Dosio and L. Cattel, *Int. J. Nanomedicine,* 2006, **1**, 297–315.
12 A. Jesorka and O. Orwar, *Annu. Rev. Anal. Chem.*, 2008, **1**, 801–32.
13 H.-I, Chang and M.-K. Yeh, *Int. J. Nanomedicine*, 2012, **7**, 49–60.
14 G. Bozzuto and A. Molinari, *Int. J. Nanomedicine*, 2015, **10** 975–999.
15 D. D. Lasic, J. J. Vallner, and P. K. Working, *Curr. Opin. Mol. Ther.*, 1999, **1**, 177–85.
16 S. Dromi, V. Frenkel, A. Luk, B. Traughber, M. Angstadt, M. Bur, J. Poff, J. Xie, S. K. Libutti, K. C.P. Li and B. J. Wood, *Clin. Cancer Res.*, 2007, **13**, 2722–2727.
17 Y. Liu, K. Li, J. Pan, B. Liu and S.-S. Feng, Biomaterials 2010, **31**, 330–338.
18 M. I. Gibson and R. K. O'Reilly, *Chem. Soc. Rev.*, 2013, 42, 7204–7213.
19 (a) P. De, S. R. Gondi and B. S. Sumerlin, *Biomacromolecules*, 2008, **9**, 1064–1070. (b) R. P. Johnson, Y.−I. Jeong, J. V. John, C.-W. Chung, D. H. Kang, M. Selvaraj, H. Suh and I. Kim *Biomacromolecules*, 2013, **14**, 1434−1443. (c) Y. Zhan, M. Goncalves, P. Yi, D. Capelo, Y. Zhang, J. Rodrigues, C. Liu, H. Tomas, Y. Li and P. He. *J. Mater. Chem. B*, 2015, **3**, 4221-4230.
20 A. Sulistio, J. Lowenthal, A. Blencowe, M. N. Bongiovanni, L. Ong, S. L. Gras, X. Zhang, and G. G. Qiao, *Biomacromolecules*, 2011, **12**, 3469–3477.
21 J. V. John, H. Park, H. R. Lee, H. Suh and I. Kim, *Eur. J. Lipid Sci. Technol.*, 2015, DOI: 10.1002/ejlt.201400396
22 J. Chen, M. Liu, C. Chen, H. Gong and C. Gao. *Appl. Mater. Interfaces,* 2011, **3**, 3215–3223.
23 H. Xiong. P. Leonard and F Seela, *Bioconjugate Chem.*, 2012, **23**, 856–870.
24 M. Li, P. De, H. Li and B. S. Sumerlin, *Polym. Chem.*, 2010, **1**, 854-859.

25 D. N. T. Hay, P. G. Rickert, S. Seifert and M. A. Firestone, *J. Am. Chem. Soc.,* 2004, **126**, 2290-2291.
26 H. Willcock and R. K. O'Reilly, *Polymer.chem.* 2010, **1**, 149-157
27 S. Qin, Y. Geng, D. E. Discher and S. Yang, *Adv. Mater*., 2006, **18**, 2905–2909.
28 C. Zhou, M, A. Hillmyer and T. P. Lodge, *Macromolecules*, 2011, **44**, 1635–1641.
29 V. Torchilin, *Adv. Drug Deliv. Rev*., 2011, **63**, 131–135.
30 R. Fanciullino and J. Ciccolini, *Curr. Med. Chem.*, 2009, **16**, 4361–4373.
31. K. Nag and V. Awasthi, *Pharmaceutics*, 2013, **5**, 542–569.

Graphical Abstract to

Folic Acid-Tethered Poly(*N*-isopropylacrylamide)–Phospholipid Hybrid Nanocarrier for Targeted Drug Delivery

Johnson V John, Young-Il Jeong, Renjith P. Johnson, Chung-Wook Chung, Huiju Park, Dae Hwan Kang, Jin Ku Cho, Yongjin Kim and Il Kim

Folic acid-tethered poly(*N*-isopropylacrylamide)-phospholipid nanocarriers exhibit tumour targetability and temperature responsive Doxorubicin releasing behaviour at physiological conditions.